24th INTERNATIONAL CONGRESS ON SOUND AND VIBRATION
23–27 July 2017, London

VIBRATION CHARACTERISTICS OF CLOSED CABS BY ENERGY FINITE ELEMENT ANALYSIS

Junchuan Niu, Zhihui Liu

Shandong University, School of Mechanical Engineering, Jinan, China
email: niujc@sdu.edu.cn

Considering of out- and in-plane waves simultaneously, energy finite element analysis (EFEA) for coupled plates are studied. The power transmission coefficients are calculated. Taking a closed car-like structure as an example, its energy flux and energy density are visualized to show the validity of the presented method.

Keywords: coupled plate, vibration, energy finite element method

1. Introduction

A growing number of light-weight structures have been used in practical engineering. These structures composed of some plates usually have the characters of high flexibility and strong coupling relationships with other structures or external circumstance, which makes the dynamic behaviors, become increasingly complex. In order to make the machineries run steadily as well as to reduce the noise level, the first thing which should be done is to find a powerful and valid dynamic prediction method for predicting the vibration of coupled plates structures.

Various dynamic prediction methods have been used to analyze the system dynamic behavior. Finite Element Method (FEM) and Statistical Energy Method (SEA) are the most widely accepted method among them. FEM has been proven to be effective and powerful at low frequency. With the increase of the frequency, both the efficiency and the accuracy of classical FEM decrease. SEA is an alternative dynamic prediction method which usually used in high frequencies range with numerous industrial applications. However, SEA characters the subsystem by one energy level only, and no spatially variation information inside the subsystem can be obtained.

Firstly proposed by Nefske and Sung [1], Energy Finite Element Analysis (EFEA) is an emerging prediction method over the past years, which attracted much attention due to its advantages of broad applicable frequency range and providing the detailed vibration information of structures. EFEA regards the space-averaged and time-averaged energy density as the primary variable and establishes the structure energy density governing equation on the basis of the energy balance of structure infinitesimal by applying the wave theory and solid mechanics relationship. The spatial variation of the dynamic response can be obtained in this way. In addition, the results given by EFEA can clearly identify the energy transfer path, which benefits the engineers to take targeted measures to cut off the energy flow into the specific area.

With years of development, the EFEA has been successfully applied to individual structure such as rod, beam, membrane, plate and acoustic cavity [2, 3]. To employ the EFEA on the coupled plates, various types of coupled plates have been investigated. Park and Hong investigate the propagation of in-plane waves in L-shaped plates [4]. Seo predicted the response of the beam-plate coupled structures using power flow analysis method [5], and Kessissoglou calculated the power flow of L-shaped plate [6]. Niu studied the rectangle L-shaped and n-shaped coupled plates considering flexural wave and in-plane wave simultaneously [7, 8]. These studies have successfully extended the EFEA to some kinds of coupled plates structures. However, these investigations are mostly based on the simple cases:

most of the studies are of the rectangle plates and the right corner coupling shape, which are far away from the coupled plates structures in practical engineering.

In this paper, the hybrid element types are introduced into the EFEA to predict the vibration of the coupled structures. Based on the wave method and reverberant wave filed assumption, the power transfer coefficients are investigated in which flexible out- and in-plane waves are considered simultaneously. A numerical simulation of car-like closed cabs is performed to exhibit the feasibility of the presented method.

2. EFEA of individual plate

The energy density governing equation of EFEA is established on the plane wave superposition principle, and the plane waves are assumed to be incoherent. When the Kirchhoff-Love plate theory is adopted, the governing equation of the plates can be written as

$$D\left(w_{xxxx}+2w_{xxyy}+w_{yyyy}\right)+\rho h\ddot{w}=F\left(x,y,t\right) \tag{1}$$

where D is the flexural rigidity of the plates, w is the displacement normal to the plate plane and its subscripts show the derivatives with respect to the relative symbols, ρ is the mass density of the plate and h is the thickness of the plate.

Many studies have been devoted to find the solution of Eq.(1), and the solutions for various types of boundary conditions have been obtained by analytical or semi-analytical method. The closed form solution of Eq. (1) for general boundary condition is unknown. One can assume a wave type solution with time harmonic and space harmonic,

$$w\left(x,y,t\right)=A_1\mathrm{e}^{\mathrm{j}k_{fx}x}\mathrm{e}^{\mathrm{j}k_{fy}y}\mathrm{e}^{\mathrm{j}\omega t} \tag{2}$$

where A_1 is the amplitude of the wave, and k_{fx},k_{fy} are the x, y components of the wave number respectively. After omitting the near field wave and time-harmonic, the wave solution for Eq. (1) can be written as

$$w(x,y)=\left(A_1\mathrm{e}^{-\mathrm{j}k_{fx}x}+A_2\mathrm{e}^{\mathrm{j}k_{fx}x}\right)\left(B_1\mathrm{e}^{-\mathrm{j}k_{fy}y}+B_2\mathrm{e}^{\mathrm{j}k_{fy}y}\right) \tag{3}$$

The energy density associated with the plate's flexural motion can be expressed in terms of the flexural displacement w as

$$e\left(x,y,t\right)=\frac{D}{2}\mathrm{Re}\left\{w_{xx}w_{xx}^{*}+w_{yy}w_{yy}^{*}+2\mu w_{xx}w_{yy}^{*}+2\left(1-\mu\right)w_{xy}w_{xy}^{*}+\rho h/D\,\ddot{w}\dot{w}^{*}\right\} \tag{4}$$

where μ is the poison ratio and the superscript "*" indicates the complex conjugation. In the Cartesian coordinate system, the x and y components of the energy intensity can be respectively calculated as

$$I_x=M_{xx}\dot{w}_x+M_{xy}\dot{w}_y-Q_x\dot{w},I_y=M_{yy}\dot{w}_y+M_{yx}\dot{w}_x-Q_y\dot{w} \tag{5}$$

where formulas of $M_{xx},M_{yy},M_{xy},M_{yx},Q_x,Q_y$ can be referred to the literature [8].

The energy density and energy intensity can be averaged both in space and time space to obtain a clear relationship between them,

$$\left\langle I\right\rangle=-\frac{c_g^2}{\eta\omega}\nabla\left\langle e\right\rangle \tag{6}$$

where c_g is the group velocity of the flexural wave. According to the energy conservation principle, the input energy is equal to the leaving and dissipating energy in a small volume,

$$-\frac{c_g^2}{\eta\omega}\nabla^2e\left(x\right)+\eta\omega e\left(x\right)=\pi_{\mathrm{in}} \tag{7}$$

where, π_{in} is the injected power in unit area. The same procedures can be implemented to obtain the energy density governing equation of the in-plane wave, which has the same math form.

Mathematically speaking, Eq.(7) is a two-order partial differential equation, which is difficult to

obtain the analytical solution. It can be solved by the Galerkin method. The quadrilateral or other elements are utilized in the processing, so the Eq. (7) is discretized as

$$\left(\boldsymbol{k}_D^e + \boldsymbol{k}_G^e\right)\boldsymbol{e}^n = \boldsymbol{b}^e + p_{\text{in}}^e \tag{8}$$

where $\boldsymbol{k}_D^e, \boldsymbol{k}_G^e$ is the stiffness matrix, $\boldsymbol{b}^e$ is the input power vector, p_{in}^e is the energy flux matrix at the boundary, $\boldsymbol{e}^n$ is the energy density which includes all the node values of the unit.

3. Power transfer coefficient of the coupled plate

To apply the EFEA on the coupled plates, the energy transmission relationship should be investigated firstly. For the coupled plates structures, the incident wave will induce other types of wave when impinging the boundary, therefore the energy of the different type of wave should be studied simultaneously. The coupled plate is schematically shown in Figure 2(a). From the standpoint of the wave propagation in the plates, when the incident wave impinges the coupling boundary the discontinuity of the coupling boundary creates the wave reflection and transmission. For the flexural wave, both the traveling wave and evanescent wave arise on the coupling boundary. The wave solution of the flexural wave and in-plane waves excluding the evanescent wave can be respectively written as

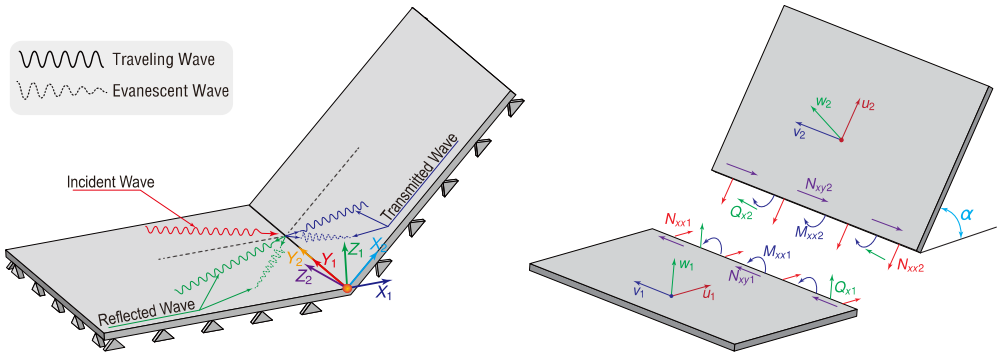

(a) (b)

Figure 2: Sketches (a) waves in coupled plate structure and (b) the coupled conditions.

$$w(x,y) = \left(A_1 e^{-\mathrm{j}k_{fx}x} + A_3 e^{\mathrm{j}k_{fx}x}\right)e^{-\mathrm{j}k_{fy}y} + \left(A_2 e^{-\mathrm{j}k_{fx}x} + A_4 e^{\mathrm{j}k_{fy}x}\right)e^{\mathrm{j}k_{fy}y} \tag{9}$$

$$\begin{aligned} u(x,y) = \cos\theta_l &\left(B_1 e^{\mathrm{j}xk_{lx}+\mathrm{j}yk_{ly}} + B_2 e^{\mathrm{j}xk_{lx}-\mathrm{j}yk_{ly}} - B_3 e^{-\mathrm{j}xk_{lx}+\mathrm{j}yk_{ly}} - B_4 e^{-\mathrm{j}xk_{lx}-\mathrm{j}yk_{ly}}\right) \\ +\sin\theta_s &\left(C_1 e^{\mathrm{j}xk_{sx}+\mathrm{j}yk_{sy}} - C_2 e^{\mathrm{j}xk_{sx}-\mathrm{j}yk_{sy}} + C_3 e^{-\mathrm{j}xk_{sx}+\mathrm{j}yk_{sy}} - C_4 e^{-\mathrm{j}xk_{sx}-\mathrm{j}yk_{sy}}\right) \end{aligned} \tag{10}$$

$$\begin{aligned} v(x,y) = \sin\theta_l &\left(B_1 e^{\mathrm{j}xk_{lx}+\mathrm{j}yk_{ly}} - B_2 e^{\mathrm{j}xk_{lx}-\mathrm{j}yk_{ly}} + B_3 e^{-\mathrm{j}xk_{lx}+\mathrm{j}yk_{ly}} - B_4 e^{-\mathrm{j}xk_{lx}-\mathrm{j}yk_{ly}}\right) \\ +\cos\theta_s &\left(-C_1 e^{\mathrm{j}xk_{sx}+\mathrm{j}yk_{sy}} - C_2 e^{\mathrm{j}xk_{sx}-\mathrm{j}yk_{sy}} + C_3 e^{-\mathrm{j}xk_{sx}+\mathrm{j}yk_{sy}} + C_4 e^{-\mathrm{j}xk_{sx}-\mathrm{j}yk_{sy}}\right) \end{aligned} \tag{11}$$

where $k_{mx} = k_m \cos\theta_m$, $k_{my} = k_m \sin\theta_m (m = f, l, s)$, $k_m (m = f, l, s)$ and $\theta_m (m = f, l, s)$ are the wave numbers and the heading angle of the m (flexural, longitudinal and shear) wave, respectively, and $A_i, B_i, C_i (i = 1, \cdots, 4)$ are the amplitudes of the waves. The exponents with positive expression represent the wave propagating to the negative direction and vice versa.

Figure 2(b) is shown the force equilibrium and displacement continuity condition when two plates are coupled together. A homogeneous matrix can be used here to express these force equilibrium and displacement compatible conditions in the same coordinates system, that is

$$\mathbf{T} = \begin{pmatrix} \cos\alpha & 0 & -\sin\alpha & 0 \\ 0 & 1 & 0 & 0 \\ \sin\alpha & 0 & \cos\alpha & 0 \\ 0 & 0 & 0 & 1 \end{pmatrix} \tag{12}$$

Then, one has the force equilibrium and the displacement compatible conditions as,

$$\mathbf{I}\cdot\mathbf{u}_1=\mathbf{T}\cdot\mathbf{u}_2 \tag{13}$$

$$\mathbf{I}\cdot\mathbf{F}_1+\mathbf{T}\cdot\mathbf{F}_2=\mathbf{0} \tag{14}$$

where $\mathbf{I}$ is the identity matrix, $\mathbf{u}_i=[u_i,v_i,w_i,\theta_i],(i=1,2)$, θ_i is the rotation angle with respect to the coupling angle, and $\mathbf{F}_i=(N_{xxi},N_{xyi},Q_{xi},M_{xxi}),(i=1,2)$.

Combination of Eq. (13) and (14) gives the relationship of the amplitude between the incident wave and other types of waves. For the linear system considered here, the amplitude of the incident wave can be set to unit to simplify the calculation, after which the amplitudes of other waves induced by incident wave can be obatined easily.

For the plane wave, the power flow towards the coupling boundary can be expressed as the multiplication of the wave group speed and energy density. The power flow of the flexural wave, longitude wave and shear wave can respectively be calculated as

$$P_f=c_{gf}e_f=\frac{\omega}{k_f}\mathrm{Re}\left(\rho h|A_{\mathrm{in}}|^2\omega^2\cos\theta_f\right) \tag{15}$$

$$P_m=c_{gm}e_m=\frac{1}{2}\frac{\omega}{k_m}\mathrm{Re}\left(\rho h|A_{\mathrm{in}}|^2\omega^2\cos\theta_m\right) \tag{16}$$

where $|A_{\mathrm{in}}|^2$ denotes the 2-norm of a specific incident wave, and $(m=f,l)$. For the coupled plates consisting of two individual plates, there are six kinds of power flow in total, including three reflection power flow and three transmission power flow.

To quantify the various kinds of power flow, the power reflection coefficients and power transmission coefficients can be calculated

$$r_{ijmn}(\theta)=\frac{P_{jn}(\theta)}{P_{im}(\theta)},t_{iimn}(\theta)=\frac{P_{in}(\theta)}{P_{im}(\theta)} \tag{17}$$

where the first subscript of the coefficient indicates the source of the incident wave, the second indicate the induced wave position, the third indicate the incident wave type and the forth the induced wave type.

The power transmission coefficients of a coupled plates consisting of two individual plates are computed here, and the parameters are set as follows: α=90°, ρ=2700kg/m^3, E=7.1×10^{10} Pa, h=1mm, ω=1.68e6rad/s, $k_l/k_f=0.3$, $k_s/k_f=0.5$, $k_l/k_s=0.6$.

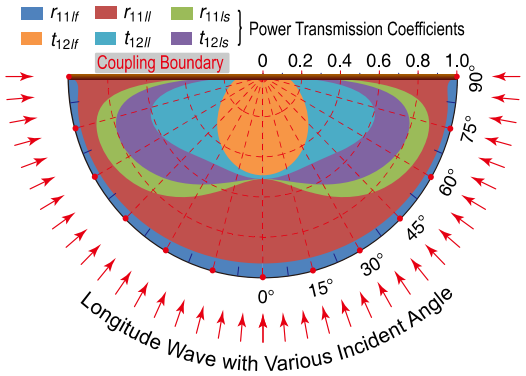

Figure 3: Transmission coefficients of the coupled plate.

From Figure 3, it can be noticed that the power transmission coefficients of the longitude wave break and disappear when the sine of the incident angle reaches 0.3. The shear wave breaks and disappears when the sine of the incident angle reaches 0.5. These breaks is corresponding to the critical wave type conversion angle since the wave number ratio of the flexural wave to longitude wave is 0.3 and that to the shear wave is 0.5, which can also be predicted by the Snell Law.

It is obvious that the power transmission coefficients vary with the incident angle. The reverberant wave field assumption, which is the main assumption of the energy finite element analysis, assume

that the wave filed is diffuse and the incoherent, so that the total power impinges the coupling boundary can be written as

$$P_{tot} = \int_{-\pi/2}^{\pi/2} P_{im}(\theta)\mathrm{d}\theta \tag{18}$$

And the total reflection and transmission power can be written as

$$P_{r,tot} = \int_{-\pi/2}^{\pi/2} r_{ijmn}(\theta) P_{im}(\theta)\mathrm{d}\theta, P_{t,tot} = \int_{-\pi/2}^{\pi/2} t_{iimn}(\theta) P_{im}(\theta)\mathrm{d}\theta \tag{19}$$

After the incident angle average, the power reflection coefficients and the power transmission coefficients can respectively be written as

$$r_{ijmn} = \frac{P_{r,tot}}{P_{tot}}, t_{iimn} = \frac{P_{t,tot}}{P_{tot}} \tag{20}$$

When the incident waves are longitude wave and shear wave, the power transfer coefficients can be obtained in the similar way.

4. Coupling relationship of the coupled plate

The power flow in the plates can be divided into two parts: the power flow toward the coupling boundary q^- and the power flow away from the coupling boundary q^+, and the energy density can be divided in the similar way. Then the total energy density and the power flow can be expressed as

$$e = e^+ + e^-, q = q^+ - q^- \tag{21}$$

For the plane waves, the energy flow can be expressed in terms of the group speed and energy density

$$q_m^+ = c_{gm} e_m^+, q_m^- = c_{gm} e_m^-, (m = f, l, s) \tag{22}$$

When the flexural wave and in-plane wave are taken into account simultaneously, any kinds of the wave can be induced by all three types of wave. Consider the power reflection and transmission as well as the wave type conversion, the power flow can be expressed as the sum of the contributions of all the wave, that is

$$\begin{aligned}
q_f^{k+} &= \tau_{(k+1)kff} q_f^{(k+1)-} + \tau_{(k+1)klf} q_l^{(k+1)-} + \tau_{(k+1)ksf} q_s^{(k+1)-} + \quad r_{kkff} q_f^{k-} + r_{rklf} q_l^{k-} + r_{kksf} q_s^{k-} \\
q_l^{k+} &= \tau_{(k+1)kfl} q_f^{(k+1)-} + \tau_{(k+1)kll} q_l^{(k+1)-} + \tau_{(k+1)ksl} q_s^{(k+1)-} + \quad r_{kkfl} q_f^{k-} + r_{rkll} q_l^{k-} + r_{kksl} q_s^{k-} \\
q_s^{k+} &= \tau_{(k+1)kfs} q_f^{(k+1)-} + \tau_{(k+1)kls} q_l^{(k+1)-} + \tau_{(k+1)kss} q_s^{(k+1)-} + \quad r_{kkff} q_f^{k-} + r_{rklf} q_l^{k-} + r_{kkss} q_s^{k-}
\end{aligned} \tag{23}$$

For another plate, the power flow can be expressed in the similar way,

$$\begin{aligned}
q_f^{(k+1)+} &= \tau_{k(k+1)ff} q_f^{k-} + \tau_{k(k+1)lf} q_l^{k-} + \tau_{k(k+1)sf} q_s^{k-} + r_{(k+1)(k+1)ff} q_f^{(k+1)-} + r_{(k+1)(k+1)lf} q_l^{(k+1)-} + r_{(k+1)(k+1)sf} q_s^{(k+1)-} \\
q_l^{(k+1)+} &= \tau_{k(k+1)fl} q_f^{k-} + \tau_{k(k+1)ll} q_l^{k-} + \tau_{k(k+1)sl} q_s^{k-} + r_{(k+1)(k+1)fl} q_f^{(k+1)-} + r_{(k+1)(k+1)ll} q_l^{(k+1)-} + r_{(k+1)(k+1)sl} q_s^{(k+1)-} \\
q_s^{(k+1)+} &= \tau_{k(k+1)fs} q_f^{k-} + \tau_{k(k+1)ls} q_l^{k-} + \tau_{k(k+1)ss} q_s^{k-} + r_{(k+1)(k+1)fs} q_f^{(k+1)-} + r_{(k+1)(k+1)ls} q_l^{(k+1)-} + r_{(k+1)(k+1)ss} q_s^{(k+1)-}
\end{aligned} \tag{24}$$

where the subscripts of the q denote the wave type. Rewrite Eq. (23) and (24) in the matrix form as

$$\boldsymbol{q}^+ = \mathbf{C} \cdot q^- \tag{25}$$

Since the power flow can be expressed as the vector sum of the power flow in two opposite directions, the net power flow entering the plate k through the coupling boundary can be expressed as

$$\begin{aligned}
q_f^k &= \tau_{(k+1)kff} c_{gf}^{(k+1)} e_f^{(k+1)-} + \tau_{(k+1)klf} c_{gl}^{(k+1)} e_l^{(k+1)-} + \tau_{(k+1)ksf} c_{gs}^{(k+1)} e_s^{(k+1)-} + \left(r_{kkff} - 1\right) c_{gf}^k e_f^{k-} + r_{kklf} c_{gl}^k e_l^{k-} + r_{kksf} c_{gs}^k e_s^{k-} \\
q_l^k &= \tau_{(k+1)kfl} c_{gf}^{(k+1)} e_f^{(k+1)-} + \tau_{(k+1)kll} c_{gl}^{(k+1)} e_l^{(k+1)-} + \tau_{(k+1)ksl} c_{gs}^{(k+1)} e_s^{(k+1)-} + r_{kkfl} c_{gf}^k e_f^{k-} + \left(r_{kkll} - 1\right) c_{gl}^k e_l^{k-} + r_{kksl} c_{gs}^k e_s^{k-} \\
q_s^k &= \tau_{(k+1)kfs} c_{gf}^{(k+1)} e_f^{(k+1)-} + \tau_{(k+1)kls} c_{gl}^{(k+1)} e_l^{(k+1)-} + \tau_{(k+1)kss} c_{gs}^{(k+1)} e_s^{(k+1)-} + r_{kkff} c_{gf}^k e_f^{k-} + r_{rklf} c_{gl}^k e_l^{k-} + \left(r_{kkss} - 1\right) c_{gs}^k e_s^{k-}
\end{aligned} \tag{26}$$

The net power flow entering the plate k+1 can be obtained in the similar manner. Rewrite Eq.(26) in the matrix form as

$$q = q^+ - q^- = \left(\mathbf{C} - \mathbf{I}\right) \cdot \mathbf{A} \cdot e^- \tag{27}$$

where $\mathbf{A}=\mathrm{diag}(c_{gf}^{k},c_{gl}^{k},c_{gs}^{k},c_{gf}^{(k+1)},c_{gl}^{(k+1)},c_{gs}^{(k+1)})$ is the group speed matrix building the relationship between the power flow and the energy density. From Eq. (21), one has

$$\mathbf{A}\cdot e=\mathbf{A}\left(e^{+}+e^{-}\right)=q^{+}+q^{-} \tag{28}$$

Substituting Eq. (25) into Eq. (28) yields

$$e=\mathbf{A}^{-1}\left(\mathbf{C}+\mathbf{I}\right)\mathbf{A}e^{-1} \tag{29}$$

If $\mathbf{A}^{-1}\left(\mathbf{T}+\mathbf{I}\right)\mathbf{A}$ is invertible, Eq. (29) can be rewritten as

$$e^{-}=\mathbf{A}^{-1}\left(\mathbf{C}+\mathbf{I}\right)^{-1}\mathbf{A}e \tag{30}$$

Substituting Eq. (30) into Eq. (27), Eq. (27) can be rewritten as

$$q=q^{+}-q^{-}=\left(\mathbf{C}-\mathbf{I}\right)\times\left(\mathbf{C}+\mathbf{I}\right)^{-1}\mathbf{A}e \tag{31}$$

Equation (31) gives the relationship between the energy density and the power flow. For the coupled plate structures, the power transfer should be considered. When the power transfer through the coupling boundary are taken into account, the finite element equation can be rewritten as

$$\mathbf{K}\cdot\boldsymbol{e}=\boldsymbol{\Pi}_{\mathrm{in}}+\mathbf{Q} \tag{32}$$

where $\mathbf{Q}$ is the power flow entering the plate through the coupling boundary, which has the same dimension as Π_{in}. When the plate is partitioned into many of the small elements, the coupling boundary is also partitioned into many of pieces. As the $\boldsymbol{q}$ in Eq. (31) is the power flow per unit length, the total power flow entering the plate through the coupling boundary can be evaluated as

$$\mathbf{Q}=\sum_{k=1}^{n}\int q_k\mathrm{d}l_k \tag{33}$$

where n is the number of the pieces of the coupling boundary. Substituting Eq. (31) and Eq. (33) into(32), the following result can be obtained,

$$\mathbf{K}\cdot\boldsymbol{e}=\boldsymbol{\Pi}_{\mathrm{in}}+\sum_{k=1}^{n}\int_{l_k}\left(\mathbf{C}-I\right)\times\left(\mathbf{C}+\mathbf{I}\right)^{-1}\mathbf{A}\cdot e_k^{cb}\mathrm{d}l_k \tag{34}$$

where $\boldsymbol{e}$ and e^{cb} are, respectively, the energy density of the element nodes and the energy density on the coupling boundary. In many cases, the plate cannot be partitioned by quadrilateral element shown as Fig.4(a), in which the hybrid elements are adopted. The coupled plates structure consists of three individual plates. The top plate is partitioned by the triangular element while others are partitioned by the quadrilateral element.

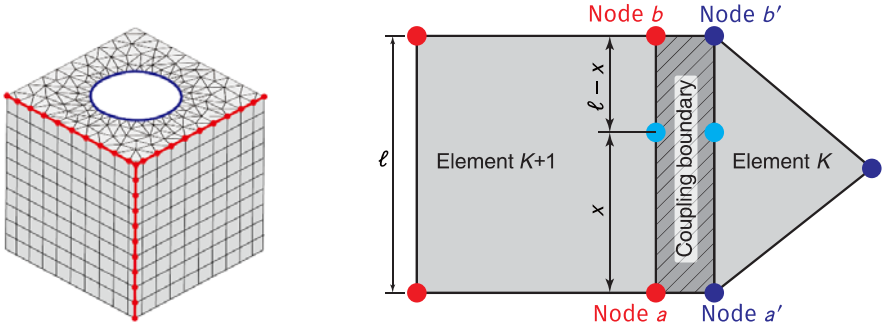

(a) (b)

Figure 4: Sketches of (a) hybrid elements in a coupled plate, and (b) combination of triangular element and quadrilateral element.

For both the quadrilateral element and triangular element, the energy density on the coupling boundary can be expressed in terms of the energy density of the nodes on the coupling boundary in the same math form, that is

$$e^{cb}=\left[(l-x)/l,x/l\right]\cdot\left[e^{a},e^{b}\right]^{\mathrm{T}}=\mathbf{R}\cdot\boldsymbol{e}^{n} \tag{35}$$

Substituting Eq. (35) into Eq. (34), the Eq (34) can be rewritten as

$$\left(\mathbf{K}-\sum_{k=1}^{n}\mathrm{S}\int_{l_k}\left(\mathbf{C}-\mathbf{I}\right)\cdot\left(\mathbf{C}+\mathbf{I}\right)^{-1}\mathbf{A}\cdot\mathbf{R}^{k}\,\mathrm{d}l\right)\cdot\boldsymbol{e}=\Pi_{\mathrm{in}} \tag{36}$$

where S is the matrix mapping the nodes number on the boundary to the global node number.

5. Numerical simulation of a car-like structure

Figure 5(a) shows a car-like coupled plates structure. This structure consists of eight plates including six rectangle plates and two irregular plates. Since the two irregular plates cannot be partitioned by the rectangular element, the triangular element is used to partition them.

A power excitation with unit amplitude $P = 1W$ is subjected to the bottom plate. Figure 5(b)-(d) show the energy density distribution and power flow fluxes of the flexural wave, longitude wave and shear wave, respectively. It can be observed that the energy density of the flexural wave reaches the highest lever at the excitation position, and decays with the increasing of the distance from the excitation position. For the longitude wave and shear wave, it can be found that the energy density reaches the highest level near the edge of the bottom plate, which is as expected since the bottom plate is subjected to flexural excitation and the in-plane waves are induced by the flexural wave when the flexural wave bounces off the edges. It can also be observed that the contour line of the flexural wave energy density is denser, indicating that the flexural wave decays more rapidly with respect to the space. It can also be predicted from the standpoint of the wave, since the flexural wave is dispersive while the in-plane waves are no-dispersive, the flexural wave has the larger wave number and the shorter wave length at high frequency, which means that the flexural wave would go through more. space period damping compared with the in-plane wave. The power flow leaves away from the excitation position and propagates to the places where the energy density is lower.

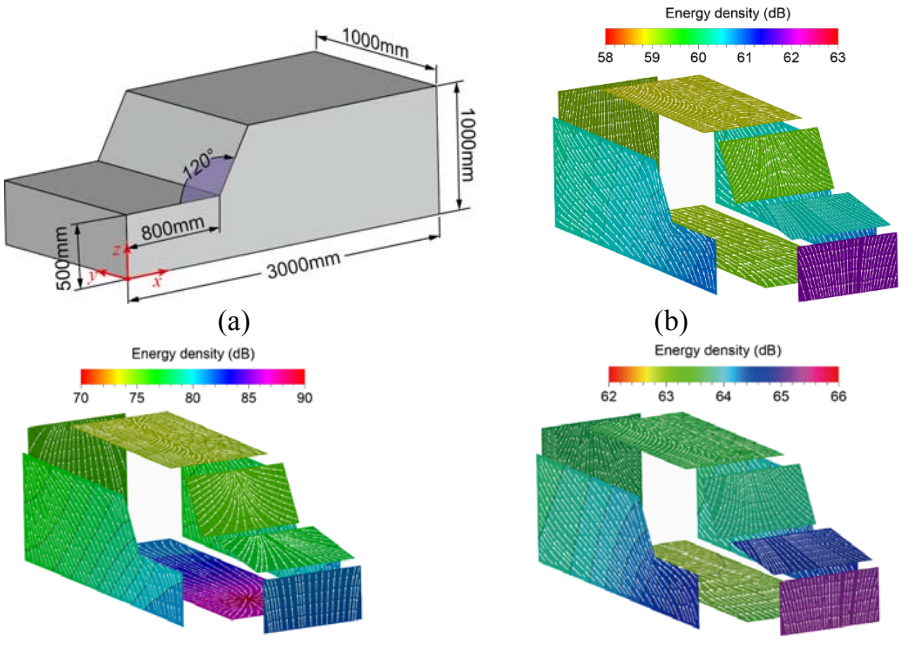

Figure 5: (a) model of car-like structure, energy density distribution and power flow of (b) flexural wave, (c) longitude wave and (d) shear wave.

6. Conclusions

Energy finite element method is developed to predict the mid-high frequencies dynamic behaviour of the coupled plate structures with the consideration of the flexural wave and in-plane wave simultaneously. Both the quadrilateral elements and the triangular elements are utilized in the finite element analysis, which make the EFEA applicable for plates with arbitrary shape. The power transmission coefficients are investigated by the traveling wave method in order to assemble the global matrix. Considering a closed car-like structure as an example, its energy flux and energy density of out- and

in-plane waves are visualized simultaneously by the proposed method, which shows that the proposed method is capable of analysing the complex coupled plate structures with all types of wave filed.

Acknowledgement

The work is supported by National Natural Science Foundation of China (No. 51675306 and No. 51275275).

REFERENCES

1 Nefske, D.J. and Sung, S.H., Power flow finite element analysis of dynamic systems: basic theory and application to beams, *Journal of Vibration, Acoustics, Stress, and Reliability in Design*, **111**(1), 94-100, (1989).

2 Cho, P. E., *Energy flow analysis of coupled structures*, PhD Thesis, Purdue University, (1993).

3 Bouthier, O. M. and Berhard, R. J., Simple models of energy flow in vibrating membranes, *Journal of Sound and Vibration*, **182**(1), 129-147, (1995).

4 Park, D. H., Hong, S. Y. and Kil, H.G., Power flow models and analysis of in-plane waves in finite coupled thin plates, *Journal of Sound and Vibration*, **244**(4), 651-668, (2001).

5 Seo, S.H., Hong, S.Y. and Kil, H.G., Power flow analysis of reinforced beam-plate coupled structures, *Journal of Sound and Vibration*, **259**(5), 1109-1129, (2003).

6 Kessissoglou, N. J., Power transmission in L-shaped plates including flexural and in-plane vibration, *Journal of Acoustical Society of America*, **115**(3), 1157-1169, (2004).

7 Niu, J. C. and Li, K. P., Energy flow finite element analysis of l-shaped plate including three types of waves, *Applied Mechanics & Materials*, **353-356**, 3365-3368, (2013).

8 Niu, J. C., Li, K. P., Energy finite element analysis of n-shaped plate structures with three types of wave, *Journal of Vibration Engineering and Technologies*, **3**(5), 615-625, (2015).